Tetrahedron Vol. 48, No. 9, pp. 1605-1616, 1992
Printed in Great Britain

0040-4020/92 $3.00+.00

NMR and Molecular Modelling Studies of two Photoproducts of 2'-Deoxy-4- thiouridylyl-(3',5')- thymidine.

Pascale Clivio, Alain Favre[§], Catherine Fontaine, Jean-Louis Fourrey*, Jeannette Gasche, Eric Guittet and Philippe Laugâa[§]

Institut de Chimie des Substances Naturelles, C.N.R.S., 91190 Gif sur Yvette, France and [§]Laboratoire de Photobiologie Moléculaire, Institut Jacques Monod, C.N.R.S., 2, Place Jussieu, 75251 Paris Cedex, France.

(*Received in Belgium* 9 *January* 1992)

Key words: 4-thiouracil photochemistry, photochemical probe, 2D NOE spectroscopy, molecular modelling.

Abstract: Preparation, spectroscopic analysis and molecular modelling of dYo(4-α;p)dT and dhs^{4}U(6-α;p)dT, two photoproducts of 2'-deoxy-4-thiouridylyl-(3',5')-thymidine are described. The 6(S) configuration of the additional chiral centre of dhs^{4}U(6-α;p)dT has been determined using 2D-NMR spectroscopy. NMR data also provided conformational information on the deoxyribose and glycosidic torsion angles of dYo(4-α;p)dT and dhs^{4}U(6-α;p)dT. The two fragments of dYo(4-a;p)dT have an anti type glycosidic conformation. The furanose conformation of the 5' -end is exclusively C3' -endo and that of -pdT is mainly C2' -endo. A syn/anti glycosidic torsion angle is found for both sugars in dhs^{4}U(6-α;p)dT. A C2' -endo/C3' -endo conformation blend exists for the 5' -furanose whereas the second sugar prefers a C2' -endo geometry. The detailed three-dimensional reconstruction of the solution state was performed using NMR guided molecular modelling.

INTRODUCTION

The development of light activated cross-linking probes as tools to decipher the various types of molecular interactions within nucleic acid (particularly RNAs) or nucleoprotein assemblies is currently receiving a great deal of interest (1-3). In general the best probes are those which show a reasonable chemical stability and whose presence causes limited perturbations into the system under study. In the field of nucleic acids the photoaffinity probes which can meet these requirements are certainly those which are closely derived from the usual nucleobases. The normal bases are indeed known to undergo a variety of photochemical reactions which have been used in various kinds of photolabelling experiments. However such applications are limited because of the low specificity of the photochemical processes (4-6). Hence as an improvement we have proposed the use of 4-thiouracil which interestingly is a naturally occurring residue found at the 8th position of a number of *E. coli* tRNAs. In these molecules 4-thiouracil can be considered as a built-in photoaffinity probe since it undergoes, upon selective 360 nm photoactivation, a coupling reaction with a distant cytosine located at the 13th position.

This reaction produces a 5-(4'-pyrimidin-2'-one) cytosine (Cyt(5-4)Pyo) derivative which presumably results from H_2S elimination of a thermally unstable primary thietane photoproduct. The formation of Cyt(5-4)Pyo in tRNA demonstrates that in this molecule the 8 and 13 residues are not only in close proximity but in a head to tail arrangement. Indeed such a spatial relationship can be deduced from the reasonable mechanism which was proposed for the above reaction on the basis of the structure of the tRNA photoproduct as well as the photochemical behaviour of 4-thiouracil derivatives in model reactions (7-11).

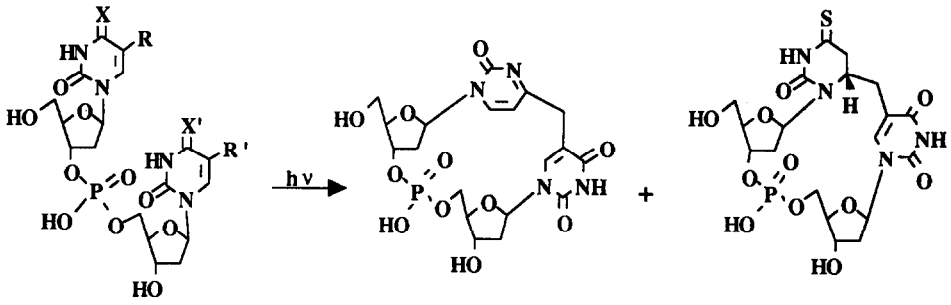

ds^{4}UpT **1** (X=S, R=H, X'=O, R'=CH_3)
dTps^{4}U **2** (X=O, R=CH_3, X'=S, R'=H)

dYo(4-α;p)dT **3**

dhs^{4}U(6-α;p))dT **4**

Figure 1. Reaction scheme for the formation of photoproducts **3** and **4** from **1** (Abbreviations are those recommended in ref. 13).

With a continued interest in developing 4-thiouracil and congeners as selective photoaffinity probes for the structural investigations of nucleic acids we have undertaken a programme to study the photochemical behaviour of 4-thiouracil when incorporated in simple oligonucleotide models. To our surprise in the case of 2'-deoxy-4-thiouridylyl-(3',5')-thymidine ds^{4}UpdT **1** and thymidylyl-(3',5')-2'-deoxy 4-thiouridine dTpds^{4}U **2** we have observed a photoreactivity dependence on the sequence of the two substrates. In particular 360 nm irradiation of ds^{4}UpdT **1** gave two products **3** and **4** (figure 1), the structural types of which have never been encountered before in nucleic acids photochemistry (12). We now report the as yet undetermined configuration assignment of **4** and the solution conformation of the two photoproducts obtained by irradiation of ds^{4}UpdT, as deduced from NMR and molecular modelling studies.

MATERIALS AND METHODS

Abbreviations and conventions: The abbreviations employed for photoproducts **3** and **4** are those proposed by Cohen et al. (13). All angle conventions used in Table 5 and 7 conform to those summarized in Saenger (14).

Irradiation and Purification: A solution of ds^{4}UpdT **1** in neutral water (0.17 mg/ml) was irradiated with a super pressure HBO 350 W lamp (335-360 nm) at 0°C under nitrogen atmosphere (bubbling). The reaction was monitored by the disappearance of the maximum at 330 nm on the UV spectrum. After completion, the solution was then concentrated in vacuo. The two photoproducts were isolated by reverse phase chromatography (RP 18) using water as eluent.

UV Spectroscopy: UV absorbance measurements were performed in H_2O at pH 7 on a Lambda Perkin-Elmer spectrometer.

Mass Spectrometry: Negative fast atom bombardment (FAB) (thioglycerol matrix) mass spectra were recorded using a Kratos MS 80 mass spectrometer.

NMR Spectrometry: NMR spectra were recorded on a Bruker AM 400 spectrometer. The samples were lyophilized twice in 99.8 % D_2O and dissolved in 400 µl of D_2O. Chemical shifts are reported relative to the internal HDO peak set at 4.8 ppm. The coupling constants were determined by a first-order analysis of the ^1H NMR spectra, along with decoupling experiments. In all 2D NMR experiments, 512 FIDs of 1024 data points were collected with a spectral width of 4000 Hz, the relaxation delay was set to 1s. The data were zero-filled once in the t_1 dimension before Fourier transformation. For the phase-sensitive 2D NOE (15) spectra, a mixing time of 400 ms was used. In the t_2 and t_1 dimensions the data points are multiplied by a $\pi/2$ shifted sine-bell. In the phase-sensitive DQF-COSY (16) the time domains were multiplied by a shifted ($\pi/4$) sine-bell before Fourier transformation. A 250 ms fixed delay was applied in the LR-COSY (17) experiments (absolute value Fourier transformation).

Molecular Mechanics: Two different approaches were retained for the three-dimensional reconstruction of the two photoproducts based on molecular mechanics. In the first one, the Macromodel program (18) was used, the energy minimization was performed with the AMBER force field. Initial structures were constructed interactively to satisfy most of the NMR parameters (NOE and vicinal couplings), restrained minimizations using distance constraints were then performed followed by an unrestrained final run. Typically 200 steps were necessary until the energy of the structures did not change any more and the gradient was sufficiently low.

A complementary approach involved the molecular mechanics calculations and graphics of the SYBYL package (Tripos Associates Inc., 1699 South Hanley Road, suite 303, Saint Louis, Missouri 63144, USA). As in the first approach the energy function used is that designed by Kollman and coworkers (19,20) to model nucleic acids and proteins. The atomic charges are from a series of Gaussian 80 UCSF calculations using a minimal STO-3G basis set. All the calculations were performed using the all-atom model, with a dielectric constant proportional to the interatomic distance and a non bonded cut-off of 12 Å. Initial geometries for dYo(4-α;p)dT **3** were built using SYBYL facilities. The following procedure was used. The dinucleotide **3** was built in three different conformations : A, B and that elicited by d(pTpT) in crystalline state (21). The photoproduct was then built in two steps, for each starting conformation. First, soft distance range and angle constraints were imposed between the thymine methyl and a dummy atom introduced at position 4 of uracil, in order to position them at best for bond closure, and minimization was performed allowing only phosphodiester backbone relaxation. Then the covalent bond was formed and extensive minimization performed on the fully relaxed structure. Since the three minimized structures were very different we decided to explore a larger conformational space. For this purpose the three minimized structures were subjected to molecular dynamics at 2000 K for 50 ps after slow warming and a 30 ps equilibration phase. Conformers were sampled every 0.5 ps and submitted to extensive minimization. All refinements were considered to be converged when the r.m.s. derivative of the energy function relative to atomic coordinate changes were smaller than 0.1 kcal/mol per Å. For each starting structure 100 conformers were obtained. All 300 conformers were sorted and grouped in conformational families according to discontinuities in the torsional angle variations. All following work deals with the 10 families of lowest energy.

dhs^{4}U(6-α;p)dT **4** was constructed in the same way but, since every family for **3** contains conformers deriving of the three starting structures, the B form only was constructed. In this case the sampling was performed every 0.25 ps during the molecular dynamics phase, generating 200 conformers.

RESULTS AND DISCUSSION

Mass Spectrometry : The negative FAB mass spectra of dYo(4-α;p)dT **3** and dhs^{4}U(6-α;p)dT **4** display an ion at m/z 513 and 547, respectively, corresponding to $(M-H)^-$.

U. V. Spectroscopy : In both cases, an ipsochromic shift from 330 nm for ds^{4}UpdT **1** to 270 nm for **3** and 276 nm for **4** is observed. This indicates the loss of the conjugated π system of the 4-thiouracil base.

NMR assignments : The structure elucidation of **3** and **4** (with the exception of the absolute configuration at carbon 6) has been published elsewhere (12).

Assignments of the proton resonances of **3** and **4** (Table 1) were performed at 400 MHz using 2D COSY techniques (1D spectra shown Figure 2). Resonances of the 3' -end and 5' -end deoxyribose protons were differentiated either from long range COSY spectra which display a connectivity between the H6 proton of the base and the H1' of its sugar (J4) or from the multiplicity of the H3' signal of the 5' -end deoxyribose which is

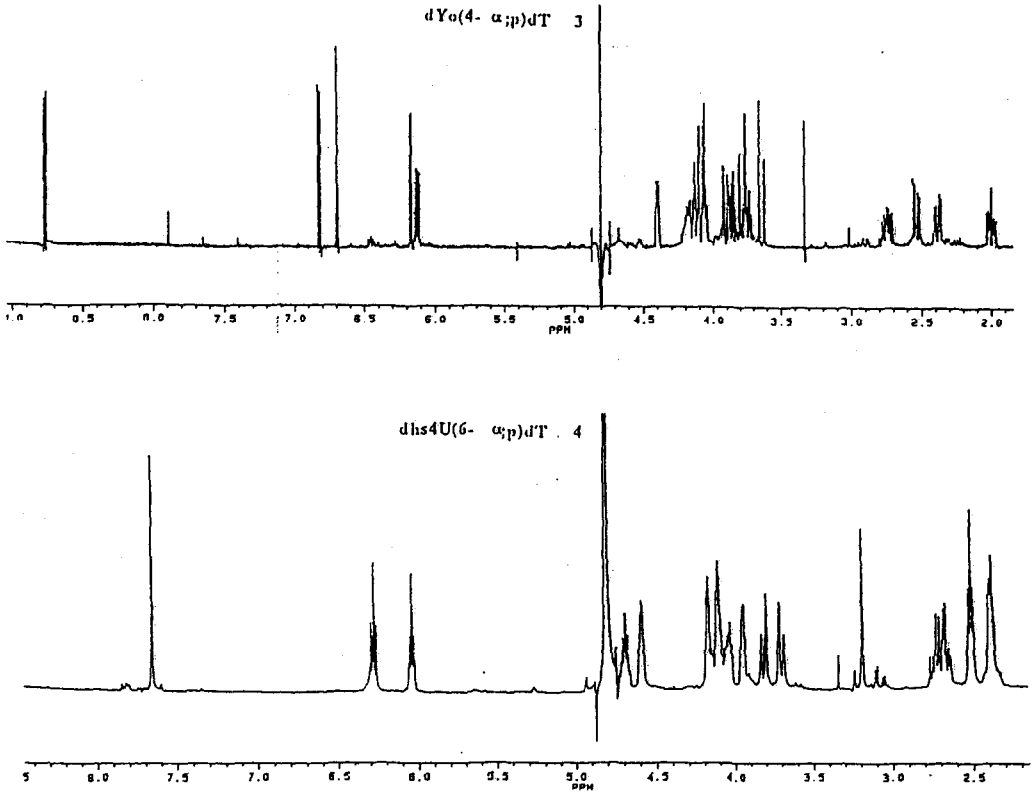

Figure 2. ^{1}H 400 MHz spectra of dYo(4-α;p)dT **3** and dhs^{4}U(6-α;p)dT **4** at 23 °C in D_2O.

coupled to the phosphorus atom. Indirect assignments of the prochiral C5' protons refer to the method of Lee *et al.* (22). The prochiral C2' protons are assigned from observed NOE between the H6 proton of the base and the H2' (2'R) or from the comparative magnitude of J1'2', J1'2", J2'3', J2"3' of various envelope conformations (23). The methylene protons of carbon C7 bridging the two pyrimidine rings of the two photoproducts are identified from their long range coupling with the H6 proton of the thymidine base. In the case of **4**, the H7 protons allow the attribution of the methine proton H6 and the methylene protons H5. These latter are exchangeable with deuterium upon long time storage in D_2O implying a thioketo-enol equilibrium at the C-4/C-5 position.

Table 1. ^1H chemical shifts in ppm (from residual HDO, 4.8 ppm) of ds^{4}UpdT **1**, dYo(4-α;p)dT **3** and dhs^{4}U(6-α;p)dT **4** at 23° C in D_2O

	ds^{4}UpdT		dYo(4-α;p)dT		dhs^{4}U(6-α;p)dT	
proton	ds^{4}Up-	-pdT	dYop-	-pdT	dhs^{4}Up-	-pdT
H1'	6.28	6.11	6.13	6.09	6.04	6.28
H2'	2.33	2.33	2.50	1.96	2.50	2.37
H2"	2.59	2.33	2.70	2.34	2.50	2.37
H3'	4.71	4.55	4.14	4.36	4.69	4.59
H4'	4.19	4.10	4.03	4.03	3.94	4.17
H5'	3.80	4.11	4.08	3.82	3.81	4.10
H5"	3.73	4.04	3.87	3.71	3.69	4.10
H5	6.47		6.79		3.07(R)*	
					3.21(S)*	
H6	7.68	7.67	8.73	6.66	4.03	7.65
CH3		1.86				
H7(R)*				3.75		2.73
H7(S)*				3.60		2.64

*: Assignment of the prochiral protons is discussed in the NOE's section.

Analysis of the coupling constants: The measured coupling constants of **1**, **3** and **4** are listed Table 2. They have been interpreted in terms of population of two puckered ^3E (C3' -endo) and ^2E (C2' -endo) modes (Table 3) following the procedure described by Cheng and Sarma (23). A value of J1'2' + J3'4' included in the interval 10.8 +/- 1 Hz indicates an equilibrium blend of ^2E and ^3E conformations. When J1'2' + J3'4' cannot be obtained, J1'2'+J1'2" can be used to provide information on the conformational equilibrium (24). In our case, with the exception of the 5' -nucleotidyl unit of **3**, all furanoses are in an equilibrium of $^2E/^3E$ conformers (Table 3). The two sugars of **1** adopt a preferential C2' -endo conformation (30% ^3E ie 70% ^2E) as the majority of deoxyribodinucleoside monophosphates. A major ^2E (C2' -endo) population (80%) is observed for the -pdT fragment of **3** whereas the J1'2' magnitude (0 Hz) indicates an exclusive ^3E conformation (ie C3' -endo) for the 5' -nucleotidyl fragment. This may result from the C4 (ds^{4}Up-) to CH2 (-pdT) linkage of the dimer. The furanose ring of the dhs^{4}Up- part of **4** is in a 50% equilibrium of ^2E and ^3E conformers. A 77% ^2E (C2' -endo) population is observed for the second sugar.

Table 2. Observed coupling constants (in Hz) of **1**, **3** and **4**.

	1		3		4	
	ds^{4}Up-	-pdT	dYop-	-pdT	dhs^{4}Up-	-pdT
J1'2'	6.5	6.8a	0	9.0	6.0a	7.0a
J1'2"	6.5	6.8a	6.2	5.2	6.0a	7.0a
J2'2"	14.2	b	13.3	14.2	b	b
J2'3'	6.5	5.3c	5.5	6.1	6.8c	4.4c
J2"3'	3.8	5.3c	11.3	1.7	6.8c	4.4c
J3'4'	3.5	3.6	*	2.2	5.5	2.5
J4'5'	3.3	*	*	5.6	2.3	*
J4'5"	4.5	4.2	3.2	7.0	3.7	*
J5'5"	12.6	12.3	13.3	10.4	12.6	*
J56	7.6		6.8		6.1(R); 0.0(S)	
J6CH$_2$7					8.2(R); 5.0(S)	
JCH$_2$7				15.7		14.6
JCH$_2$5						18.2
J3'P	6.5		*		5.5	
J5'P		*		5.6		*
J5"P		4.2		7.0		*

a: J=(J1'2'+J1'2")/2

b: Due to close magnetic equivalence of the two C2' protons at 400 MHz individual spin-coupling constants could not be determined

c: J=(J2'3'+J2"3')/2

*: undetermined

The angles O5'-C5'-C4'-C3' (γ) and P-O5'-C5'-C4' (β) can be obtained from the individual couplings or using the J4'5'+J4'5" and the J5'-^{31}P+J5"-^{31}P sums respectively, when the individual couplings can not be extracted (23). The 5' -nucleotidyl unit of the three compounds shows a preference for the gg conformer around the C(4')-C(5') bond (+sc domain, γ=60°) (61% for **1**, 98% for **3** and 79% for **4**). This result is in accordance with that found in deoxyribodinucleoside monophosphates (23). In the case of **3**, the population of the gg conformer at the 3' -end is 11%. Due to chemical shifts degeneracies, the same analysis could not be performed on **4**. dYo(4-α;p)dT **3** is the only photoproduct amenable to such a detailed analysis of the rotamers around the C(5')-O(5') bond due to severe overlaps in all other cases. The population of the g'g' conformer (ap domain, β=180°) is found to be 60%. The gauche trans arrangement (g't') (+sc domain, β=60°) is excluded from structural hindrance. So 40% of trans gauche population (t'g') (-sc domain, β=300°) must exist.

2D NOE spectroscopy: 2-D NOESY experiments were performed to determine the relative configuration of the carbon C6 of the saturated base of **4** as well as to obtain conformational information on the photoproducts and on the starting material **1**. The measured NOEs are listed in Table 4. They all correspond to positive NOEs,

the cross- and auto-peaks (at 400 MHz) having opposite signs, which allows to rule out spin diffusion artefacts in our analysis.

Table 3. Population distribution of conformers of the sugar of ds^{4}UpdT **1**, dYo(4-α;p)dT **3** and dhs^{4}U(6-α;p)dT **4**.

	Nucleotide	J1'2'+J3'4'	J1'2'+J1'2"	% ^{3}Ea
1	ds^{4}Up-	10.0	13.0	32
	-pdT	*	13.6	33
3	dYop-	*	6.2	100**
	-pdT	11.2	14.2	20
4	dhs^{4}Up-	*	12.0	51
	-pdT	*	14.0	23

a: calculated by using J1'2'+J3'4'=10.8 Hz and the observed magnitude of J3'4' (23)

*: impossible to calculate due to magnetic equivalence of H2', H2" or because J3'4' could not be measured.

**: determined from the J1'2' value.

An important structural aspect is the conformation about the glycosidic bond. Depending on whether the deoxyribose ring adopts a C2' -endo or a C3' -endo conformation, close proximities between the H6 protons and the H2' or H3' sugar protons are indicative of an ANTI conformation. Conversely an NOE between the base proton and the H1' proton is characteristic of a SYN conformation. The following conclusions can be drawn from the measured NOEs (Table 4):

The two glycosyl bonds of **1** are in a syn/anti equilibrium as shown by NOEs between H6-H1' and H6-H2' (from the C2' -endo conformer) and H6-H3' (from the C3' -endo conformer). Observable NOEs in **3** seem to indicate an exclusive anti conformation of the glycosyl bond of the two sugars and confirm the population equilibrium obtained from the coupling constants. The presence of a H6-H3' correlation (absence of any H6-H2' correlation) fits the C3' -endo conformation of the 5' -end sugar. The presence of H6-H2' and H6-H3' cross-peaks is in accordance with the favoured anti conformation of the second sugar and demonstrates a certain amount of flexibility within the 3' -deoxyribose. The absence of H6-H1' NOE in both fragments sustains further the anti geometry. These results are also in agreement with the molecular model which shows the inhibition of the rotation about the two glycosyl bonds and the preferable anti conformation. A NOE is observed between H5 and one of the prochiral protons H7; the glycosidic bond of the 5' -nucleotidyl part being anti, this proton H7 can be assigned to the pro(R) one.

In **4**, the first important question to address is the configuration at carbon 6 of the 5' -end base. The proton H6 of the saturated base at 4.03 ppm displays many intra and internucleoside dipolar couplings. Most of them can be satisfied by either a C6(R) or a C6(S) configuration but the observed H6-H5' (intranucleoside) and H6-H2' (internucleoside) contacts can only be reconciled with a C6(S) configuration since severe interactions cannot be avoided for all the other geometries satisfying the NMR parameters Thus, we retain the S stereochemistry for carbon 6. Several NOEs indicate some degree of motion inside the molecule: in particular, the observed intraresidue NOEs between the H6 protons and the H1', H2' and H3' protons both reflect a syn/anti equilibrium of the glycosyl bond and an equilibrium blend of the ^{2}E/^{3}E conformations of the two sugars.

Table 4. Summary of NOE's in the two photoproducts and in **1**.

Intranucleoside NOEs

	5' -nucleotide			3' -nucleotide		
	1	3	4	1	3	4
H6-H1'	p	a	p	p	a	p
H6-H2'	p	a	p1	p1	p	p1
H6-H2"	a	a	p1	p1	a	p1
H6-H3'	p	p	p	p	a	p
H6-H5'	a	a	a	a	a	p2
H6-H5"	p	a	a	a	p	p2
H1'-H2'	a	a	p1	p1	a	p1
H1'-H2"	p	p	p1	p1	p	p1
H1'-H4'	p	a	p	p	p	p
H2'-H3'	p	p	p1	p1	p	p1
H2"-H3'	a	a	p1	p1	a	p1
H2'-H4'	a	a	p1	p1	a	p1
H2"-H4'	p	a	p1	p1	a	p1
H3'-H4'	p	a	p	a	p	p
H3'-H5'	a	a	p	p	a	p2
H3'-H5"	p	a	p	p	p	p2

Internucleoside NOEs

4	3
H6 dhs^{4}Up--CH$_2$7	H5 dYop--H7(R)
H6 dhs^{4}Up--H2'H2"* -pdT	
H6 dhs^{4}Up--H6 -pdT	
H1' dhs^{4}Up--H5'H5"* -pdT	
H1' dhs^{4}Up--H6 -pdT	
H2'H2"* dhs^{4}Up--H6 -pdT	
H3' dhs^{4}Up--H6 -pdT	
H5(S)-H7(S)	

p: present, a: absent

1: H2' and H2" are isochrone

2: H5' and H5" are isochrone

*: isochrone

The absence of vicinal coupling between the H6 proton and the H5 proton observed at 3.21 ppm indicates an orthogonal spatial arrangement of these two protons. Thus, this H5 proton is pro(S). It is worth noting that the pro(R) H5 proton is more rapidly exchanged in D_2O than the pro(S) one. Observation of a molecular model shows that the thiocarbonyl group is in the same plane as the pro(S) H5 proton and approximately perpendicular to the fast exchangeable pro(R) proton. Related results have been reported for the keto-enol equilibrium where the rate of exchange of the proton in the plane of the carbonyl function is slower than that of the other one (25). The pro(S) H7 proton is assigned from its NOE with the pro(S) H5 proton.

Structure generation and refinement

dYo(4-α;p)dT 3

NMR parameters demonstrate dYo(4-α;p)dT **3** to be fairly rigid with a predominance of a conformer characterized by a C3' -endo 5' -end deoxyribose, a C2' -endo 3' -end deoxyribose, anti bases and a gauche-

trans orientation of the C(4')-C(5') bond. This geometry was fully analyzed using molecular modelling. First an interactive construction of the molecule was performed and the structure was then refined until complete relaxation. At the outcome of the run the final structure was checked against the various NMR parameters and a close agreement verified.

A more sophisticated approach was also applied, based on the use of molecular dynamics as a mean for exploring the conformational space. The detailed procedure is described in the Material and Methods section. The most salient conclusions are the following: the structural parameters of the 10 families of lowest energy are listed in Table 5. It is noteworthy that both glycosidic torsion angles of all conformers are in the anti domain and that the furanose conformation of dYop- is always C3' -endo. The pucker of the 3' -end deoxyribose is either in the C3' -endo domain (I, II, VI, IX, X) or in the C2' -endo domain (III, IV, V, VII, VIII), ranging from C1' -exo to C2' -endo. While torsion angles ε and ζ are always in the - ac range, α, β, γ show greater differences among the families. NMR data show that both bases are in the anti conformation and that the 5' -end deoxyribose sugar is exclusively in the C3' -endo conformation, with which molecular calculations agree. The high level of rigidity of the dYop residue is underlined by the narrow range of values for χ and the pseudorotational angle P ($-180 < \chi < -168$, $-2 < P < 14$), whatever the pucker of the 3' -deoxyribose is. The latter has been shown to be 80% C2' -endo, which strongly suggests that **3** should belong to either family III, IV, V, VII or VIII.

Torsion angles O5'-C5'-C4'-C3' (γ) and P-O5'-C5'-C4' (β) have been estimated from NMR scalar coupling data. At the level of the inter-residue linkage γ is 11% gg (γ=60°) based on the NMR measurements. All three possibilities are found by molecular mechanics : gg (III, VIII) ; gt (ap domain, γ=180°) (V, VII) and tg (-sc domain, γ=300°) (IV). With respect to β, NMR data have been interpreted as a 60% g'g' (180°) population and a 40% t'g' (300°) population, the g't' (60°) being excluded on a steric basis. Molecular calculations show that, for all selected families but VIII, β is in the g'g' range (in VIII β is in the t'g' range) in agreement with the NMR data. Taken together these results show that the most likely conformation of **3** belong to family IV, V or VII.

NMR NOE provide distance data. For each representative of the ten families, relevant inter-proton distances have been measured. Observed NOEs can be accounted for by a blend of families IV and V. Family VII, which differs from V by the χ value of dT only (149 versus -157) appears to be less satisfactory with regard to the NOE data. Figure 3 shows a representative member of family IV.

Table 5. Energy and torsion angles computed for dYo(4-α;p)dT **3**.

	E	χ U	χ T	P U	P T	ε	ζ	α	β	γ
I	-26.0	-172	-155	6	37	-98	-95	66	95	-75
II	-24.7	-175	-151	5	55	-101	-71	-179	-100	42
III	-24.5	-171	-178	8	135	-98	-73	-68	-172	52
IV	-22.3	-169	-150	8	161	-99	-88	58	172	-72
V	-21.9	-172	-157	5	130	-103	-75	164	176	179
VI	-19.7	-168	-144	13	42	-95	-76	101	180	-172
VII	-19.5	-172	149	5	148	-102	-73	174	179	-178
VIII	-18.9	180	-161	-2	130	-105	-78	-163	-86	66
IX	-18.4	-171	-171	5	15	-101	-88	48	166	-76
X	-18.1	-170	-128	14	47	-89	-54	-57	-175	-42

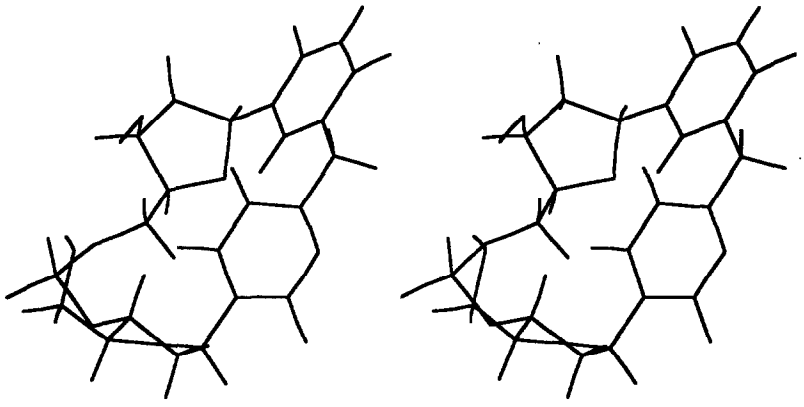

Figure 3. Stereoview of dYo(4-α;p)dT **3** as determined by molecular dynamics (Family IV).

dhs^{4}U(6-α;p)dT 4

By contrast dhs^{4}U(6-a;p)dT **4** clearly demonstrates a certain degree of internal motion involving both the sugar puckering and the glycosidic linkage. This makes a three-dimensional reconstruction of the molecule more difficult. However, inspection of various structures that could fit in part the NMR data while having a low overall energy demonstrates that a fixed spatial arrangement of the two bases can be maintained, which fits the measured coupling constants within the interbase linkage (C5-C6-C7) and NOEs. The flexibility then preferentially affects the deoxyriboses, the glycosidic linkage and the phosphate geometries. One of the energy minimized structures is presented Figure 4.

The molecular dynamics approach has also been applied to **4**. The overall flexibility of the adduct as evidenced by the NMR parameters is reflected in the large scattering of the conformational angles obtained since the 200 minimized conformers generated by the high temperature dynamics run match nearly all conformational possibilities. Unsurprisingly, none of the minimized structures listed in table 6 is able to satisfy all NOE data underlining the impossibility to bring a static description of **4**.

Therefore short dynamic runs at 300 K were performed on the 10 lowest energy conformers. They all show the great flexibility of the molecule whose 5' -residue easily undergoes a syn-anti interconversion of the glycosidic linkage, whereas both sugars repucker and yield a continuum from C3' endo to C2' endo, which agrees with the collected NMR data. However, the glycosidic linkage of the 5' -residue remains anti to high-anti.

Checking the dynamic runs at 300 K against the NMR data shows that they can be accounted for by structure **4**. A dynamic picture of **4** is summarized in Table 6. Dynamic data show that the glycosidic linkage of the 5' -residue oscillates between syn and anti, whereas that of the 3' -residue covers the whole anti domain. Since a NOE is observed between H6 and H1' of this residue we have monitored this inter-proton distance. It

appears that the H6-H1' distance ranges from 2.6 to 4 Å; thus the presence of such a NOE is consistent, for this molecule, with an anti conformation. The sugar of both residues goes back and forth between the C3' -endo and the C2' -endo domains. Analysis of the torsion angle δ as a fonction of time in terms of a C2' - C3' endo equilibrium shows that the 5' -residue sugar can be described as a 60% C2' -endo form (50% by NMR) and the 3' -residue as a 80% C2' -endo form (77% by NMR). These results show a good agreement between the molecular dynamics approach and the NMR study.

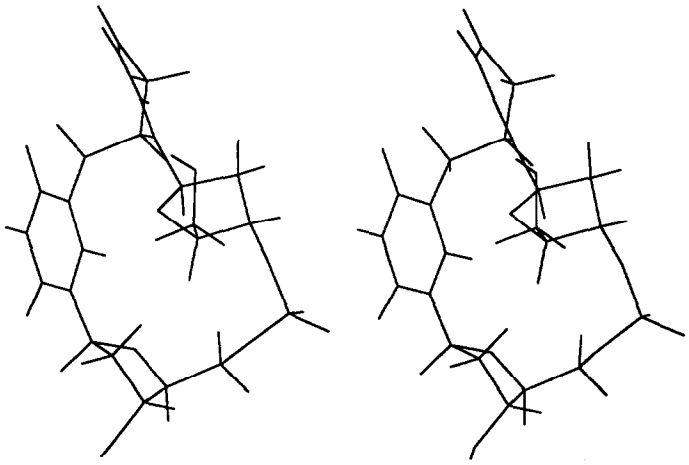

Figure 4. Stereoview of one representative conformer of dhs^{4}U(6-α;p)dT **4**.

Table 6. Range covered by the conformational angles of dhs^{4}U(6-α;p)dT **4**.

	Low	High	Mean	St dev.
χ U	1	141	70	31
χ T	-242	-88	-163	38
δ U	97	142	128	7
δ T	65	178	142	22
ε	-107	-39	-71	14
ζ	67	170	129	26
α	33	148	73	22
β	-216	-130	-172	19
γ	-208	-137	-178	16

CONCLUSIONS

The three-dimensional reconstruction of the two photoproducts **3** and **4** of 2'-desoxy-4- thiouridylyl-(3',5')- thymidine has been performed through NMR guided molecular modelling. The two photoproducts exhibit structural features which so far have not been encountered in nucleic acid constituent photochemistry. Among the important structural features of the photoproducts one should note a significant increase of the C3' -endo conformation of the 5' -end deoxyribose and a concomitant decrease of the C2' -endo conformation of the 3' -end deoxyribose, as compared to the parent dinucleotide and the predominant anti geometry of the bases in dYo(4-α;p)dT **3**. One of the adducts (**3**) is a rather rigid molecule and the three-dimensional reconstruction is fairly straightforward, whereas internal motions in the second photoproduct prevent such a detailed analysis.

Hopefully, the present study will be helpful in elucidating structures which might be encountered after irradiation of oligonucleotides containing sulfur modified nucleobases.

REFERENCES

1 Starzyk, R. (1985) *TIBS* 10, 44-45.
2 Hanna, M. M. (1989) in Dahlberg, J. F. and Abelson, J. N. (ed.), Methods in Enzymology. Academic Press, San Diego, Vol. 180,pp 383-418.
3 Branch, A. D., Benenfeld, B. J., Paul, P. P., Robertson, H. D. (1989) Ibid., 180, 418-443.
4 Sheltar, M. D. (1980) *Photochem. Photobiol. Rev.* **5**, 105-197.
5 Guerier-Takada, C., Lumelsky, N., Altman, S. (1990) *Science* **246**, 1578-1584.
6 Downs, W. D., Cech, T. R. (1990), *Biochemistry* **29**, 5605-5613.
7 Favre, A., (1990) in Morrison, H. (ed.) Photochemistry and the Nucleic Acids. John Wiley and Sons, New-York, Vol. 1,pp 379-425.
8 Favre, A., Yaniv, M., Michelson, A. M. (1969) *Biochem. Biophys. Res. Commun.*, **37**, 266-271.
9 Bergstrom, D. F., Leonard, N. J. (1972) *Biochemistry* **11**, 1-9.
10 Fourrey, J.-L. , Jouin, P., Moron, J. (1973) *Tetrahedron Lett.* 3225-3228.
11 Fourrey, J.-L., Jouin, P., Moron, J. (1974) *Tetrahedron Lett.* 3007-3008.
12 Fourrey, J.-L., Gasche, J., Fontaine, C., Guittet, E., Favre, A. (1989) *J. Chem. Soc., Chem. Commun.* 1334-1336.
13 Cohen, W. E., Leonard, N. J., Wang, S. Y. (1976) In Wang, S. Y. (ed.), Photochemistry and photobiology of Nucleic Acids. Academic Press, New-York,Vol. I, pp 403-413.
14 Saenger, W. (1984) In Cantor, C. R. (ed.), Principles of Nucleic Acid Structure. Springer-Verlag, New-York, pp 9-28.
15 Macura, S., Ernst, R. R. (1980) *Molecular Physics* **41**, 95-117.
16 Piantini,U., Sorensen, O. W. and Ernst, R. R. (1982) *J. Amer. Chem. Soc.*, **104**, 6800-6801.
17 Bax, A. and Freeman, R. (1981) *J. Magn. Res.*, **44**, 542-561.
18 Still, W. C., Richards, N. G. J., Guida, W. C., Lipton, M., Liskamp, R., Chang, G. and Hendrickson, T. Macromodel V1.5, Department of Chemistry, Columbia University New-York, NY 10027.
19 Weiner, S. J., Kollman, P. A., Nguyen, D. T., Case, D. A. (1986) *J. Comput. Chem.*, **7**, 230-252.
20 Weiner, S. J., Kollman, P. A., Case, D. A., Singh, U. C., Ghio, C., Alagona,G., Profeta, S., Weiner, P. (1984) *J. Amer. Chem. Soc.*, **106**, 765-784.
21 Camerman, N., Fawcett, J.K., Camerman, A. (1976) *J. Mol. Biol.*, **107**, 601-621.
22 Lee, C.-H., Ezra F. S., Kondo, N. S., Sarma, R. H., Danyluk, S. S. (1976) *Biochemistry*,**15**, 3627-3639.
23 Cheng, D., Sarma, R.,H. (1977) *J. Amer. Chem. Soc.* , **99**, 7333-7348.
24 Altona, C., Sundaralingam ,M. (1973) *J. Amer. Chem. Soc.*, **95**, 2333-2344.
25 Deslongchamps ,P. (1983) In Baldwin,J. E. (ed.), Stereoelectronic Effects in Organic Chemistry. Pergamon Press, Oxford, Vol. I, pp 274-277.